

Corrosion Protection of CNTs/CNFs Modified Cement Mortars

Christina V. Panagiotakopoulou, Panagiotis Papandreopoulos, George Batis

Department of Chemical Engineering, National Technical University of Athens, Athens, Greece

Email: chpanagiotak@gmail.com, panpapandr@gmail.com, batis@chemeng.ntua.gr

How to cite this paper: Panagiotakopoulou, C.V., Papandreopoulos, P. and Batis, G. (2022) Corrosion Protection of CNTs/CNFs Modified Cement Mortars. *Journal of Materials Science and Chemical Engineering*, 10, 1-17.

<https://doi.org/10.4236/msce.2022.108001>

Received: July 30, 2022

Accepted: August 28, 2022

Published: August 31, 2022

Copyright © 2022 by author(s) and Scientific Research Publishing Inc. This work is licensed under the Creative Commons Attribution International License (CC BY 4.0).

<http://creativecommons.org/licenses/by/4.0/>



Open Access

Abstract

The aim of this study is to examine the performance of nano additives in two different sets of mortar specimens armed with reinforcing steel rebars. In particular, three sets of reinforced concrete cylinders with additives of 0.1% wt of carbon nanotubes (CNTs) and carbon nanofibers (CNFs) have been exposed to a solution of 3.5% NaCl, and further examined for the impact of nano-modification on corrosion performance. The anti-corrosive performance of these additives was investigated through linear polarization technique (LPR), mass loss and mercury porosimetry technique (MIP). From the investigation results, it is found that the addition of CNTs/CNFs causes lower steel corrosion, whereas the pore structure of concrete with CNTs/CNFs can significantly reduce the mass loss rate and the relative permeability.

Keywords

Nano Additives, CNTs/CNFs, Cement Mortars, Corrosion Resistance, Electrochemical Measurements, Porosimetry

1. Introduction

Reinforced concrete is the most popular, effective and widely used material in the construction industry for over 100 years. However, for several decades, one of the most prejudicial factors for the service life of the reinforced concrete structures, and responsible for degrading its operational life, is the corrosion of steel reinforcement. In addition, the type of corrosion with the most harmed results is chloride-induced steel corrosion, which begins when the chloride ions overcome the depassivation limit of the steel, initiating the corrosion process of the steel rebars [1] [2] [3] [4] [5].

Considering the extremely high cost which is spent annually for the remediation of corrosion damages, extensive research focused on the evaluation and pre-

diction of concrete corrosion, as well as the development of complex materials with high-performance mechanical properties, such as increased strength and durability, with the aim of improving durability and safety of concrete structures operational life.

During recent decades carbon nanotubes (CNTs) and carbon nanofibers (CNFs) characterized as the most promising materials of the century due to their exceptional mechanical, electrical, chemical and thermal properties, therefore, become widely used in an extensive range of engineering and industrial applications.

Carbon nanotubes (CNTs) are allotropes formats of carbon atoms with a cylindrical nanostructure having a diameter of nanometer and their length in micrometers with the same characteristics as tubes of single or multiple layers of graphite sheets with nanosized diameters [6]. They are used as additives in the reinforcing materials, because they eliminate the cracks at the nanoscale, minimize the capillary stresses, and consequently improve the mechanical properties and consequently the service life of the concrete elements [6] [7] [8] [9].

In addition to the carbon nanotubes (CNTs) which are widely used in several nanotechnology applications, carbon nanofibers (CNFs) have also gained popularity in the building industry, mainly to enhance plain concrete's ductility, flexural toughness and strength, light weight, high corrosion and fatigue resistance, whereas their electro conductive, facilitate the communication through concrete interfaces [10].

The excellent reinforcing and toughening efficiency of CNTs and CNFs is related to the significant improvement of the critical stress intensity factor/fracture toughness, critical strain energy and the critical crack tip opening displacement. In addition, CNFs seem to have similar improvements to CNTs in terms of enhanced tensile strength, flexural strength and crack resistance [11] [12] [13].

With the view to examining for the impact of CNTs and CNFs in anti-corrosive performance and taking into consideration that the corrosion rate is the key parameter for evaluating the rate of deterioration and predicting the remaining service life of reinforcement structures, the research community focused on electrochemical techniques that measure the corrosion rate of steel in reinforced mortar.

Among several destructive and non-destructive test methods for measuring the corrosion rate, the linear polarization technique seems the most promising nondestructive, electrochemical method, which can provide a direct evaluation of the corrosion performance, and the relative instantaneous corrosion rate, which is the actual rate of corrosion mechanism [14] [15] [16] [17].

Moreover, considering also the characterization of the pore structure, the most commonly used technique is the mercury intrusion porosimetry technique (MIP), which provides features data of the pore space related to the different physical properties of the materials. This is a well-known robust method, based on the intrusion of a non-wetting fluid (mercury) into porous structures under increasing pressure, and provides information for the pore size diameter, pore size distribution, pore structure, specific surface area and pore volume. The technique is based on the capillary law governing liquid penetration into small pores and

the assumption that a non-wetting liquid can only intrude pores under pressure and that pores have cylindrical geometry. Applying the above considerations, the pore cavity to pore throat ratio and the distribution of pore cavity sizes, associated with pore throat sizes can be calculated [18] [19] [20] [21] [22].

The current study meant to define the dispersion effect of nano additives 0.1% wt CNTs and 0.1% wt CNFs in the corrosion resistance and provide information regarding the corrosion rate of the steel reinforcement.

2. Materials and Methods

The experimental process for the evaluation of the corrosion impact proceeded through electrochemical measurements, more specifically through half-cell potential, linear polarization technique, and consequently via mass loss calculations, while the corrosion environment is 3.5% NaCl solution.

Apart from the electromechanical measurements, the characterization of the pore structure is carried out by mercury porosimetry technique, which is further applied to define the impact of the nano additives of 0.1% wt CNTs and 0.1% wt CNFs in the pore system and internal structure of mortar specimens which have been exposed in corrosion environment of 3.5% NaCl solution for a 20 month's period.

2.1. Materials and Sample Preparation

For the experimental process of this study eighteen mortar cylinder specimens of 100 mm height with axially embedded steel bars of 10 mm diameter were constructed.

The following **Figure 1** presents the mortar cylinder specimen.

The slabs were made from mortar of Portland cement CEM I and for all types of specimens the aggregate used is of maximum size of 5 mm. Tap water is also used. The bars were embedded up-side down in the molds and are set of steel type of B500C.

In particular, the chemical composition of the ordinary Portland concrete is presented in **Table 1**.

The specimens have been sorted in three sets of six specimens, with a different

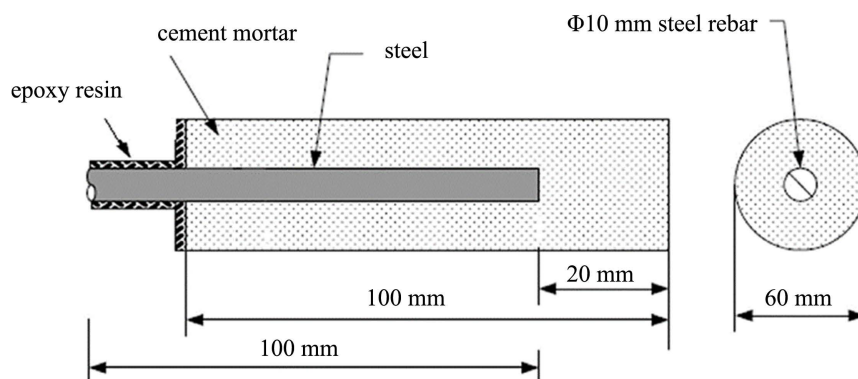


Figure 1. View of cement mortar cylinder specimen.

mortar synthesis as follows:

- Category I: Six specimens with no additives.
- Category II: Six specimens of CNT 0.1 wt%.
- Category III: Six specimens of CNF 0.1 wt%.

The characteristic properties of the nano reinforcement (CNTs and CNFs) presented in **Table 2** and **Table 3**.

Values of an estimated fiber count, the number of fibers, in this case CNTs and CNFs, which are theoretically distributed in a unit volume of the matrix, assuming perfect dispersion according to ACI 544 R-96 [23].

All specimens are stored in the laboratory room (20°C, 100% humidity) and are partially immersed up to 50% of their height in 3.5% NaCl solution for a period of 20 months.

Table 1. Chemical composition of OPC.

Constituents	Percentage
SiO ₂	20 - 67
Al ₂ O ₃	4 - 99
Fe ₂ O ₃	3 - 18
CaO	63 - 30
MgO	2 - 73
K ₂ O	0 - 37
Na ₂ O	0 - 29
SO ₃	2 - 44
LOI	1 - 52
IR(ISO)	0 - 21
CaO	2 - 41

Table 2. Properties of carbon nanotubes (CNTs) and carbon nanofibers (CNFs).

Type	Diameter (nm)	Length, (μm)	Purity (%)	Surface area, (m ² /g)	Bulk density, g/cm ³	Aspect ratio
CNTs	20 - 45	≥10	>98	>200	≤0.18	307
CNFs	100	50 - 200	-	43	0.016 - 0.148	1250

Table 3. Amount and fiber count of CNFs and CNTs of each group of specimens.

Categories	CNFs	CNTs	Fiber Count
Ref (Category I)	-	-	-
Category II	-	0.1 wt%	3.61 * 10 ¹¹
Category III	0.1 wt%	-	1.69 * 10 ¹⁰

2.2. Half-Cell Potential Measurements

In particular, information given by half-cell potential measurements is qualitative, and cannot provide information for the corrosion kinetics.

From the half-cell potential values, it can be resulted whether the corrosion is in an active or in a passive state [24]. More specifically, based on the ASTM C876-87 standard, corrosion status and the relative corrosion potential values are presented in **Table 4** as follows [25].

Considering the above, if the corrosion potential changes negatively, then corrosion rate increases.

2.3. Linear Polarization Technique

Linear polarization technique (LPT), applied for a period of 20 months in eighteen cement mortar specimens and provide information for the corrosion current (I_{corr}) for the tested samples.

The electrochemical measurements conducted regularly on a monthly basis, at standard conditions, with the aid of embedded steel as the working electrode, while an Ag/AgCl stick used as the reference electrode of the experiment, enabling the corrosion potential between the steel reinforcing bar and the auxiliary electrode to be measured.

In particular, the experimental devices used for the electrochemical measurements are the following:

- A potension meter connected to a PC.
- The reference electrode is Ag/AgCl.
- The liquid solution is distilled water with 3.5% in NaCl.
- The working electrode is Carbon (C).
- The software used is Power Suit.

Linear Polarization technique commonly used to provide information for the corrosion potential measurements, and corrosion current assessment.

Moreover, following the state of corrosion in corroding metal, linear polarization measurements, provide also information for the corrosion current at the actual time of measurement.

2.4. Mass Loss

One of the most popular test methods for defining the actual corrosion impact in the steel rebar is the weight loss measurements.

Table 4. Corrosion potential values/corrosion status [25].

Half-cell potential (mV)	Corrosion status
$E_{corr} > -200$ mV	Passive corrosion status/non-corrosive (90% probability)
-200 mV $> E_{corr} > -350$ mV	Unstable corrosion status
$E_{corr} < -350$ mV	Active corrosion status/corrosive (90% probability)

The mass loss for each rebar can theoretically be calculated by using the results of the linear polarization measurements, and the following equation which is based on Faraday's Law.

$$\beta = I * t * M / ne * F$$

β : the mass consumed due to corrosion (mg).

I : Current corresponding to the exposure time (mA).

t : Time of exposure (sec).

M : the atomic weight of Fe = 0.056 mg.

ne : 2, the ionic change (2 for $\text{Fe} \rightarrow \text{Fe}^{2+} + 2e^-$).

F : 96,500, the Faraday value.

2.5. Mercury Porosimetry Technique

In particular, the instrument used for the porosimetry technique is named as porosimeter which employs a pressurized chamber to force mercury to intrude into the voids in a porous substrate.

The device is equipped with two low-pressure ports for measuring pores in the range of macropores down to 3.5 μm and a high-pressure port for measuring pores from 6 μm down to 5 nm, reaching a maximum pressure of 33,000 psia (~2275 bar), while the three mortar samples are of 1 cm^3 volume per each tested category.

Mercury porosimetry is carried out by implementing a Micromeritics® Auto-Pore IV 9500 porosimeter. The measurement procedure consists of two main stages. In the beginning, samples and sample holders (penetrometers) are conditioned in order to desorb any traces of humidity and/or gases.

For this reason, porosimetry samples and penetrometers are normally placed for an hour inside a furnace stabilized at 110°C. Samples are previously cut into appropriate fragments in order to be adequately accommodated within the penetrometer and weighted until the desired quantity is reached.

For the initial (low pressure) measurement stage, the penetrometer is loaded in a low-pressure port where the sample is evacuated until a vacuum level below 50 μmHg (*i.e.* 6.67×10^{-5} bar) is reached and maintained for 10 minutes. This step is essential to remove gases from the porous network that may interfere with the measurement by imposing back pressure to the advancing mercury front, registering thus falsely the pores in smaller sizes. When the first stage terminates (after the vacuum stage, about 10 min are required for the measurement), the penetrometer is removed from the measuring port and then weighted in order to record the amount of total mercury that filled the penetrometer at the given pressure of 0.54 psia (*i.e.* ~37 mbar).

Subsequently, the penetrometer is loaded in the high-pressure chamber to characterize the fraction of smaller pores. After the measurement termination, a report with the results is automatically produced [25] [26].

3. Measurement and Results

The measurements and results of the above applied methods are presented as

follows.

3.1. Half-Cell Potential Assessment

The corrosion behavior of the three different sets of mortar samples are estimated by monitoring the Half-cell potential against the exposure time.

The relative diagram for the three different mortar sets is presented as follows.

From **Diagram 1**, it is found that from the 1st month of exposure all specimens were in an active corrosion status. Moreover, during the first four months of exposure, specimens in Category II and III delayed the onset of corrosion while specimens in Category I found in an active corrosion rate.

Moreover, after the 5th month of exposure, all specimens reach to a more stable E_{corr} value ranging between -650 mV and -500 mV, therefore, corrosion rate was in an active state in all tested samples until the end of the tested period. The probes with additive CNTs have the greatest half-potential.

3.2. Corrosion Current Assessment

The corrosion current, versus the exposure time of the three different categories of specimens are presented as follows.

Based on **Diagram 2**, all specimens are in an active corrosion status, while the corrosion rate in all specimen categories was low. More specific, the corrosion resistance of specimens with CNF's nano composites is found higher compared to the corrosion resistance of specimens with CNT's.

3.3. Calculated Mass Loss or Rebars

By applying on Faraday's Law, it is found that the total mass loss in each category of specimens due to corrosion impact is presented in **Table 5**.

Moreover, the mass loss per each category of the three mortar specimens, against

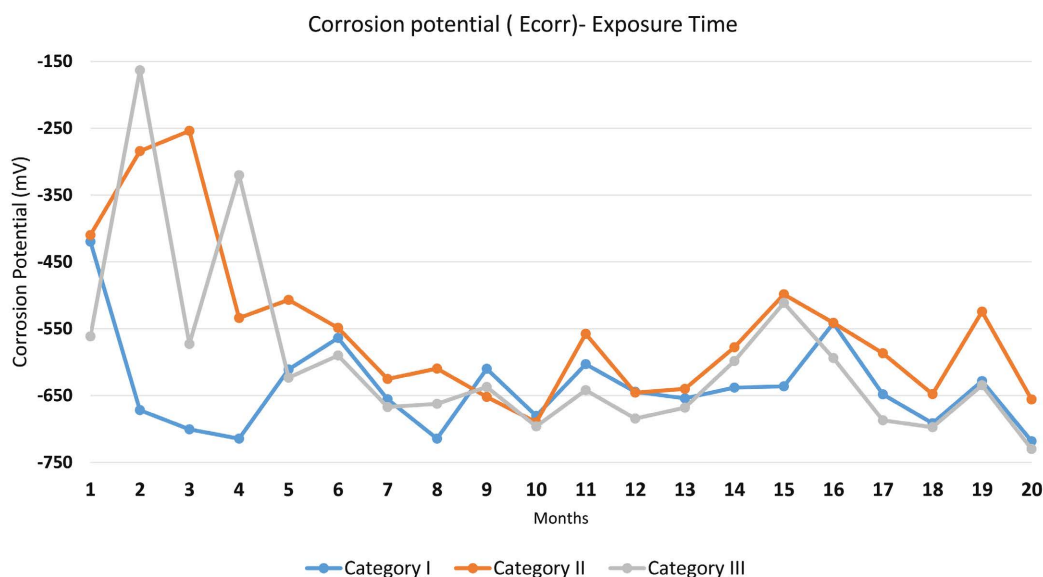


Diagram 1. Mean value of half cell potential (E_{corr})—Exposure time.

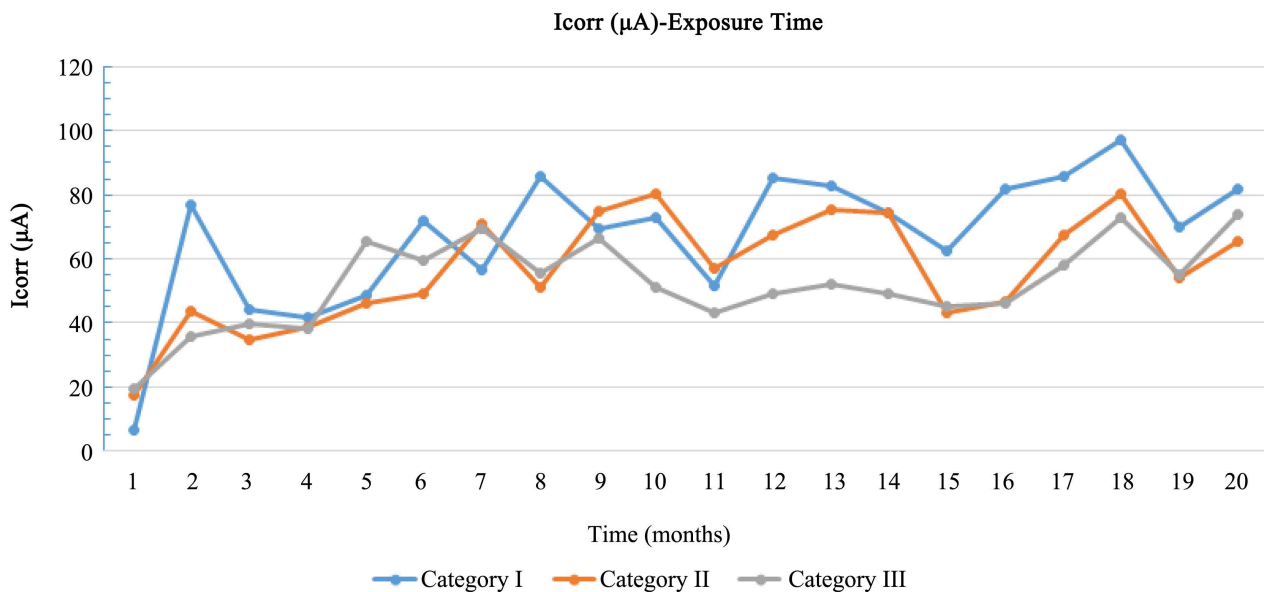


Diagram 2. Mean value of current corrosion (I_{corr})—Exposure time.

exposure time is presented in **Diagram 3**.

From the above results, it is concluded that Category III (with CNFs) lost less mass than the other two categories, due to corrosion impact. Whereas the specimens of Category II (with CNTs) lost less mass than these of Category I with no nano additives.

3.4. Mercury Porosimetry Results

The diagrams of the mercury porosimetry measurements presented as follows.

3.4.1. Category I

The mercury porosimetry of Category I specimens without nano composites results (**Diagrams 4-6**).

3.4.2. Category II

Diagrams 7-9 present the mercury porosimetry results of the specimens Category II with CNT's nano composites.

3.4.3. Category III

The mercury porosimetry results of specimens of Category III with CNF's nano composites presented in **Diagrams 10-12**.

Moreover, the diagrams for Cumulative Pore Area vs pore size and Cumulative Pore Area vs Pressure for all categories are presented as follows.

With consideration to diagrams (**Diagram 4, Diagram 6, Diagram 7, Diagram 9, Diagram 10** and **Diagram 12**) it is noted that the Cumulative intrusion (ml/gr) of Category III, considering the pore size and the applied pressure, is less than the other two categories.

From **Diagram 13** and **Diagram 14**, it is also found that the cumulative pore area (m^2/gr) considering the pore size and the applied pressure of Category III, is

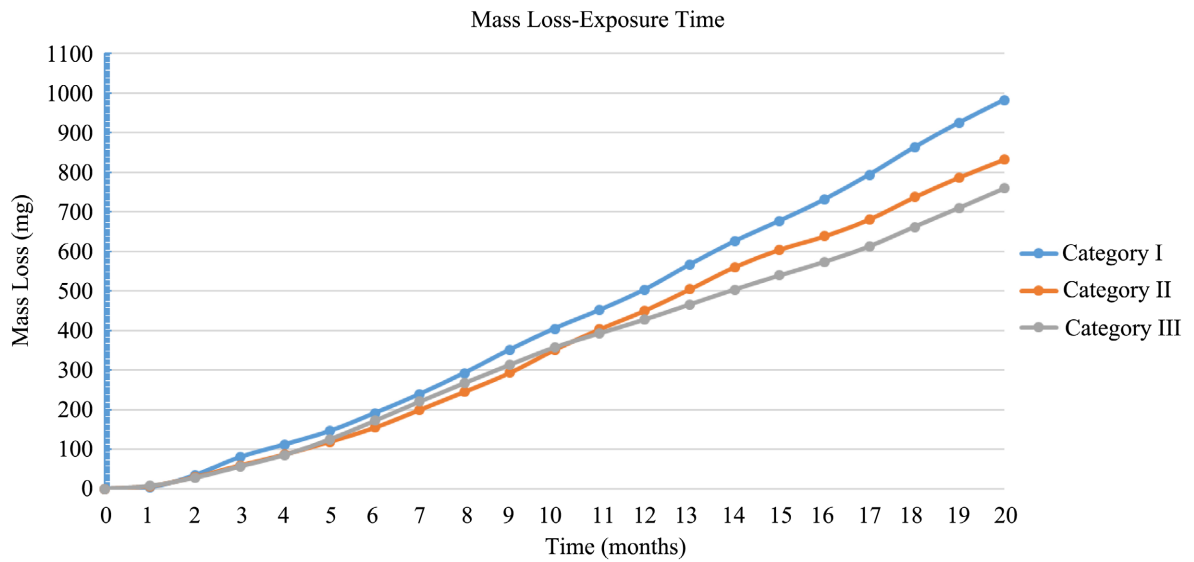


Diagram 3. Mass loss—Exposure time.

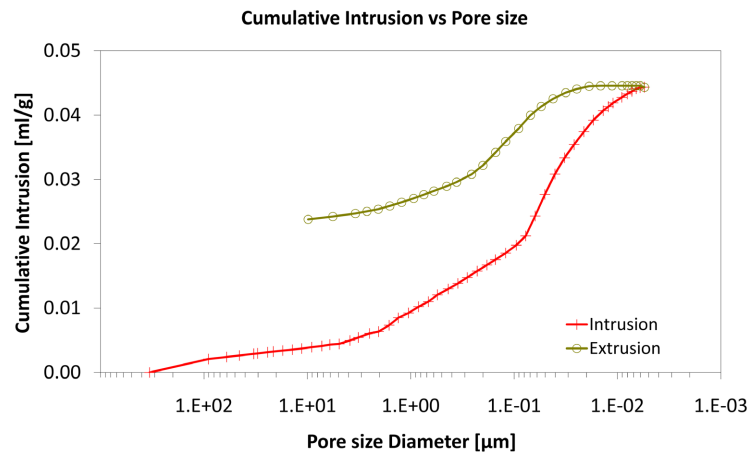


Diagram 4. Cumulative intrusion vs pore size.

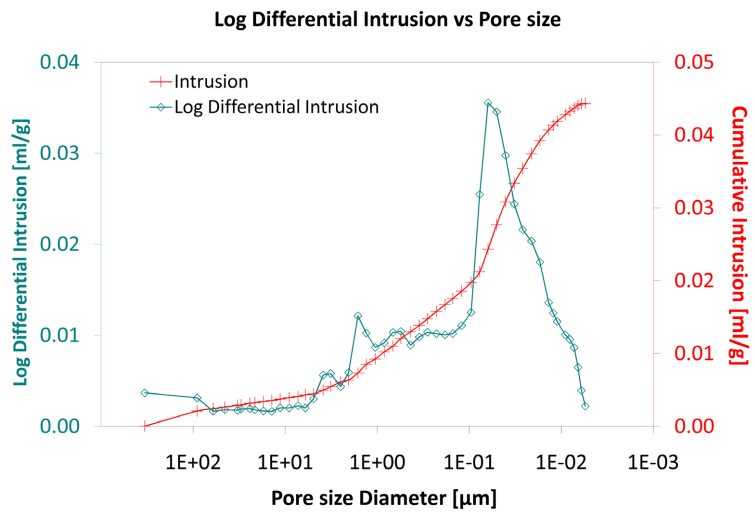


Diagram 5. Log differential intrusion vs pore size.

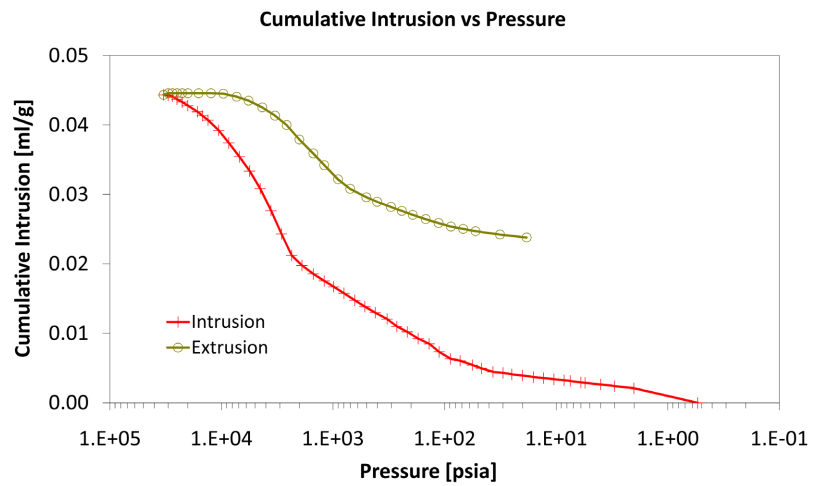


Diagram 6. Cumulative intrusion vs pressure.

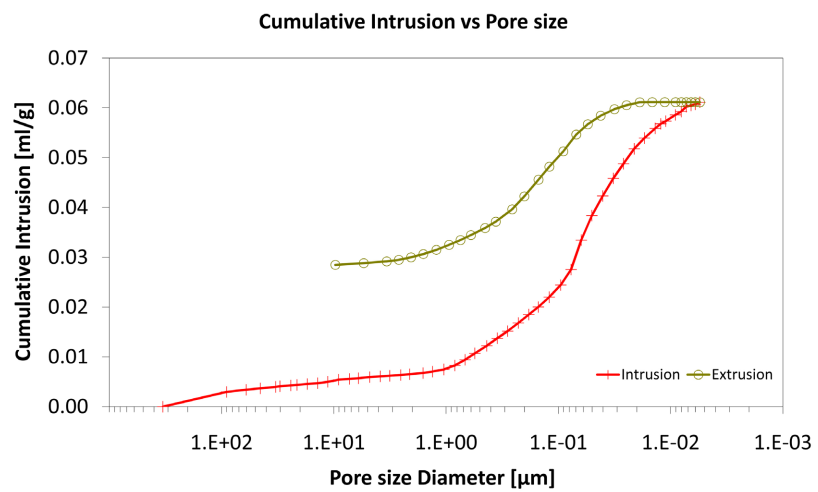


Diagram 7. Cumulative intrusion vs pore size.

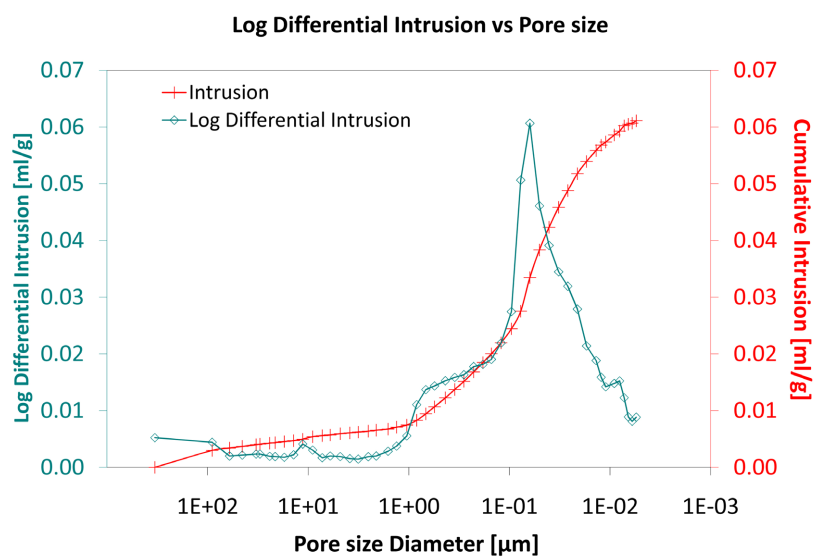


Diagram 8. Log differential intrusion vs pore size.

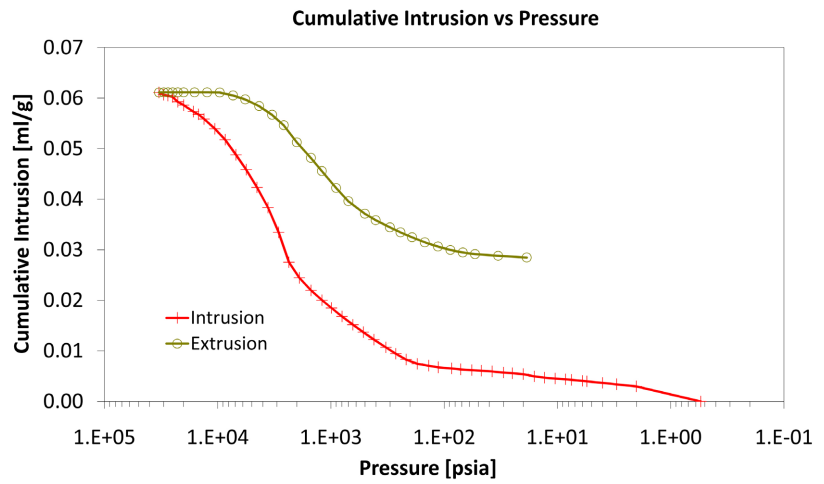


Diagram 9. Cumulative intrusion vs pressure.

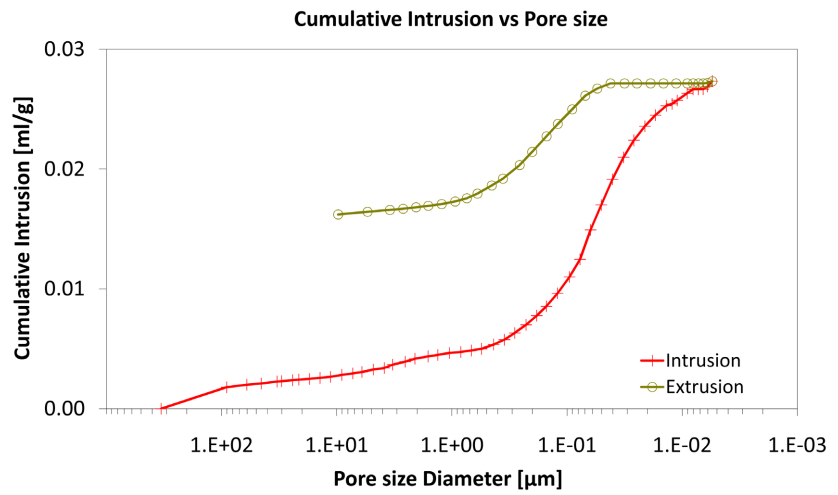


Diagram 10. Cumulative intrusion vs pore size.

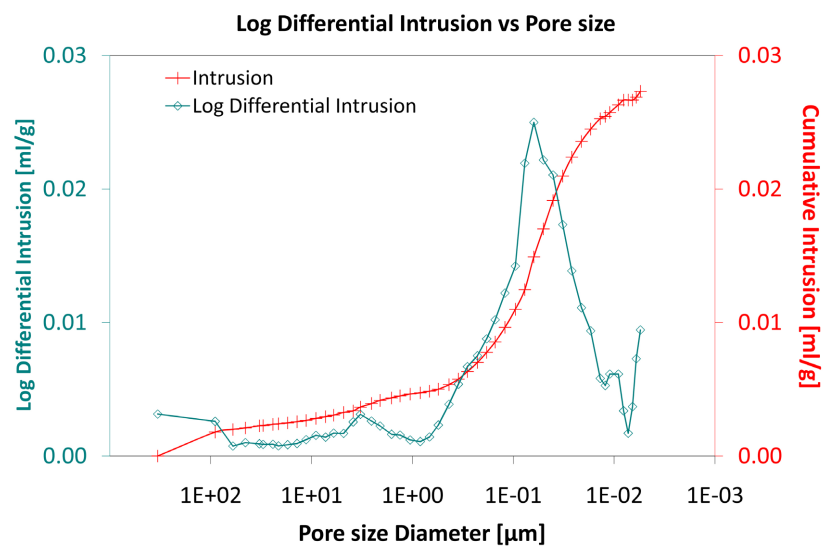


Diagram 11. Log differential intrusion vs pore size.

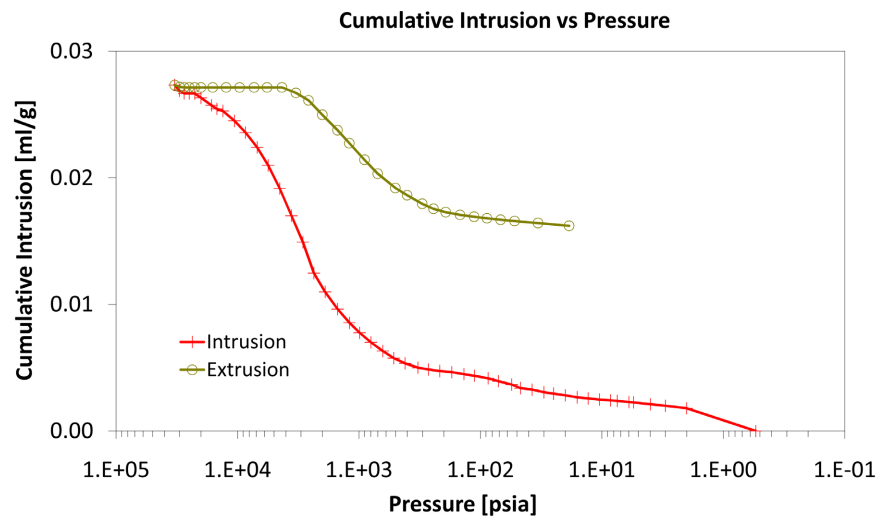


Diagram 12. Cumulative intrusion vs pressure.

Table 5. Calculated mass loss per each category.

Category of Specimens	Calculated mass loss (mg)
Category I	981.97
Category II	831.98
Category III	758.51

less than the other two categories.

Considering the log differential intrusion of Category III, in relation to the pore size diameter, it is also found less than the other two categories (**Diagram 5**, **Diagram 8** and **Diagram 11**).

Regarding the other two categories, it is noted that Cumulative intrusion (ml/gr) of Category II, considering the pore size and the applied pressure (**Diagram 4**, **Diagram 6**, **Diagram 7** and **Diagram 9**) is more than Category I. Furthermore, based on the **Diagram 13** and **Diagram 14**, the cumulative pore area (m^2/gr) considering the pore size and the applied pressure of Category I, is less than in the Category II.

Also, the log differential intrusion of Category II, considering the pore size diameter, is more than Category I (**Diagram 5** and **Diagram 8**).

Moreover, **Table 6** summarizes the values of the most characteristic sizes. Based on the above results, it is concluded that specimens in Category III meets the lower value in every tested characteristic. In particular, total intrusion volume, total pore area, porosity and stem volume are significant low comparing to other specimen categories. It is also noted that porosity (%) value of Category III is the half comparing to the Category I.

It is well known that the electrical conductivity of cement based material is a crucial factor in the corrosion of steel in mortar and concrete. In particular, upon increase of electrical conductivity, the corrosion rate also increases. Considering

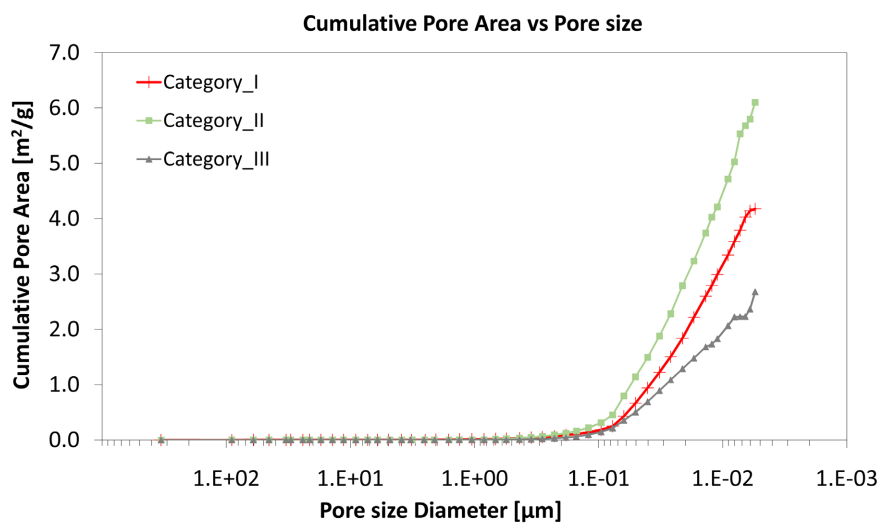


Diagram 13. Cumulative pore area vs pore size.

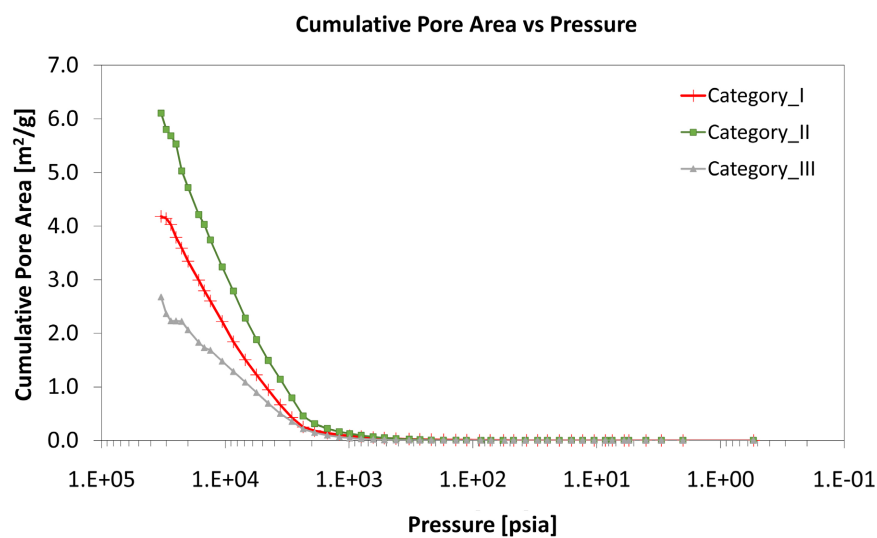


Diagram 14. Cumulative pore area vs pressure.

Table 6. Values of the most characteristic sizes from MIT measurements.

Tested Parameters	Category		
	Category I	Category II	Category III
Total Intrusion Volume (ml/g)	0.0611	0.0443	0.0273
Total Pore Area (m ² /g)	6.104	4.178	2.676
Bulk Density at 0.54 psia (g/mL)	2.1232	2.2462	2.3482
Apparent (skeletal) Density (g/mL)	2.4397	2.4946	2.5092
Porosity (%)	12.9727	9.9562	6.4165
Stem Volume Used (%)	47	52	25

the additives of CNTs/CNFs, these are found to increase the electrical conductivity, whereas, on the other hand, decrease the porosity and consequently decrease the corrosion rate.

In the present study, three different types of mortar specimens with 0.1% wt additives of CNTs and CNFs were studied regarding their protection level against corrosion by chloride ions, which is the most critical type of corrosion in steel bars of mortar structures. For the assessment of the corrosion performance electrochemical parameter such as the corrosion potential, the corrosion current density and the electrochemical mass loss were investigated, therefore the test results show that corrosion rates are affected by the addition of CNTs and CNFs to Portland cement mortars and protected the embedded steel. The result of mercury porosimetry agreed with this point of view.

The above conclusions seem to result in the common agreement with the findings of Konsta-Gdoutos *et al.* [11] who reported that the addition of 0.1% wt CNTs and CNFs increases the corrosion resistance of steel in mortars. Furthermore, the findings of Shi *et al.* [27] who reported that the incorporation of CNTs/CNFs affects the electrical conductivity of cement-based materials are also confirmed with the results of the current study.

The above results, meet also with the findings of Hassan *et al.* [28] where it is assumed that CNTs have higher corrosion tendency compared to plain concrete. It is mentioned that the results of this paper come from a very accelerated test of anodic charge, where one portion of steel was exposed to corrosion environment.

Considering the porosimetry results, based on the current study, it is assumed that the specimens of CNFs additives, result in a lower value in the total intrusion volume, total pore area, porosity and stem volume compared to other specimen categories. These results meet agreement with the findings of Shi *et al.* 3 who reported that the incorporation of CNTs/CNFs affects the microscopic characteristics and deformation of cement-based materials, and in particular, CNTs/CNFs can fill the cracks and pores in the cement matrix resulting in lower porosity and denser materials.

In regard to the permeability effect, the results of this study meet with the findings of Wang *et al.* [29], who reported that CNF can be incorporated to reduce the permeability of concrete.

Considering the findings of Del Carmen Camacho *et al.* [30], the current study concludes with the opposite result that the addition of CNT could imply the development of higher levels of corrosion in aggressive conditions. It should be highlighted that the specimens of the Del Carmen Camacho's study are made of cement paste, while the specimens of the present study are made of mortar. Also the specimens of the Del Carmen Camacho's study were covered with a paste cement cover of 6 mm, whereas the present specimens are covered with a cover layer of 25 mm mortar.

4. Conclusions

The above experiments, aim to present an assessment of the corrosion rate de-

termination, therefore, the statistical analysis of the test results it is found a significant impact of the nano additives against corrosion while exposure to extremely corrosive conditions.

In particular, based on the above analysis, the main conclusions can be drawn:

- 1) The presence of CNFs and CNTs decreased the rate of corrosion compared with the samples with mortar without nano components.
- 2) CNFs and CNTs decreased the porosity of cement mortars. This reduction remains despite the 20 months' stay in a chloride environment.
- 3) CNFs have a better performance than CNTs.

Conflicts of Interest

The authors declare no conflicts of interest regarding the publication of this paper.

References

- [1] Broomfield, J. (1997) Corrosion of Steel in Concrete Understanding, Investigation and Repair. E & FN Spon, London, 16-21. <https://doi.org/10.4324/9780203414606>
- [2] Shi, J.J. and Ming, J. (2017) Influence of Defects at the Steel-Mortar Interface on the Corrosion Behaviour of Steel. *Construction and Building Materials*, **138**, 118-125. <https://doi.org/10.1016/j.conbuildmat.2017.01.007>
- [3] Zafeiropoulou, T., Rakanta, E. and Batis, G. (2011) Performance Evaluation of Organic Coatings against Corrosion in Reinforced Cement Mortars. *Progress in Organic Coatings*, **72**, 175-180.
- [4] Broomfield, J.P. (2006) Corrosion of Steel in Concrete: Understanding, Investigation and Repair. 2nd Edition, CRC Press, Boca Raton.
- [5] Batis, G., Rakanya, E., Tsampras, L., Mougiakos, S. and Agnantiary, G. (2000) Corrosion of Reinforcing Steel. *Archive of Association of Civil Engineers of Greece*, **208**, 24.
- [6] Philip, B. (1996) The Perfect Nanotube. *Nature*, **382**, 207-208. <https://doi.org/10.1038/382207a0>
- [7] Anzar, N., Hasan, R., Tyagi, M., Yadav, N. and Narang, J. (2020) Carbon Nanotube—A Review on Synthesis, Properties and Plethora of Applications in the Field of Biomedical Science. *Sensors International*, **1**, Article ID: 100003. <https://doi.org/10.1016/j.sintl.2020.100003>
- [8] Konsta-Gdoutos, M.S., Metaxa, Z.S. and Shah, S.P. (2010) Highly Dispersed Carbon Nanotube Reinforced Cement Based Materials. *Cement and Concrete Research*, **40**, 1052-1059. <https://doi.org/10.1016/j.cemconres.2010.02.015>
- [9] Konsta-Gdoutos, M.S., Metaxa, Z.S. and Shah, S.P. (2010) Multi-Scale Mechanical and Fracture Characteristics and Early Stage Strain Capacity of High Performance Carbon Nanotube/Cement Nano-Composites. *Cement and Concrete Research*, **32**, 110-115. <https://doi.org/10.1016/j.cemconcomp.2009.10.007>
- [10] Rauti, R., Musto, M., Bosi, S., Prato, M. and Ballerini, L. (2019) Properties and Behavior of Carbon Nanomaterials When Interfacing Neuronal Cells: How Far Have We Come? *Carbon*, **143**, 430-446. <https://doi.org/10.1016/j.carbon.2018.11.026>
- [11] Konsta-Gdoutos, M.S., Batis, G., Danoglidis, P.A., Zacharopoulou, A.K., Zacharopoulou, E.K., Falara, M.G. and Shah, S.P. (2017) Effect of CNT and CNF Loading

- and Count on the Corrosion Resistance Conductivity and Mechanical Properties of Nanomodified OPC Mortars. *Construction and Building Materials*, **147**, 48-57. <https://doi.org/10.1016/j.conbuildmat.2017.04.112>
- [12] Afzal, M.T. and Khushnood, R.A. (2021) Influence of Carbon Nano Fibers (CNF) on the Performance of High Strength Concrete Exposed to Elevated Temperatures. *Construction and Building Materials*, **268**, Article ID: 121108. <https://doi.org/10.1016/j.conbuildmat.2020.121108>
- [13] Yazdani, N. and Mohanam, V. (2014) Carbon Nano-Tube and Nano-Fiber in Cement Mortar: Effect of Dosage Rate and Water-Cement Ratio. *International Journal of Material Science*, **4**, 45. <https://doi.org/10.14355/ijmsci.2014.0402.01>
- [14] Sadowski, L. (2010) New Non-Destructive Method for Linear Polarization Resistance Corrosion Rate Measurement. Wroclaw University of Technology, Wroclaw.
- [15] Stern, M. and Geary, A.L. (1957) Electrochemical Polarization: I. A Theoretical Analysis of the Shape of Polarization Curves. *Journal of the Electrochemical Society*, **104**, 56-63. <https://doi.org/10.1149/1.2428496>
- [16] So, H.S. and Millard, S.G. (2007) On-Site Measurements on Corrosion Rate of Steel in Reinforced Concrete. *ACI Materials Journal*, **104**, 638-642.
- [17] Velu, S. (2007) Corrosion Monitoring of Reinforced Concrete Structures—A Review. *International Journal of Electrochemical Science*, **2**, 1-28.
- [18] Benavent, D., Such-Basanez, I., Cortes, A.F., Pla, C., Amoros, D.C., Canaveras, J.C. and Moral, S.S. (2021) Comparative Analysis of Water Condensate Porosity Using Mercury Intrusion Porosimetry and Nitrogen and Water Adsorption Techniques in Porous Building Stones. *Construction and Building Materials*, **288**, Article ID: 123131. <https://doi.org/10.1016/j.conbuildmat.2021.123131>
- [19] Hall, C. and Hoff, W.D. (2003) Water Transport in Brick, Stone and Concrete. CRC Press, London. <https://doi.org/10.4324/9780203301708>
- [20] Abell, A.B., Willis, K.L. and Lange, D.A. (1999) Mercury Intrusion Porosimetry and Image Analysis of Cement-Based Materials. *Journal of Colloid and Interface Science*, **211**, 39-44.
- [21] Rübner, K. and Jacobs, F. (2002) Studies in Surface Science and Catalysis. Characterization of Porous Solids VI. Elsevier, Amsterdam.
- [22] Moro, F. and Bohni, H. (2002) Ink-Bottle Effect in Mercury Intrusion Porosimetry of Cement-Based Materials. *Journal of Colloid and Interface Science*, **246**, 135-149. <https://doi.org/10.1006/jcis.2002.8335>
- [23] American Concrete Institute (1996) Report on Fiber Reinforced Concrete ACI 544.1R-96.
- [24] Kouril, M., Novak, P. and Bojko, M. (2006) Limitation of the Linear Polarization Method to Determine Stainless Steel Corrosion Rate in Concrete Environment. *Cement & Concrete Composites*, **28**, 220-225. <https://doi.org/10.1016/j.cemconcomp.2006.01.007>
- [25] Scrivener, K., Snellings, R. and Lothenbach, B. (2016) A Practical Guide to Microstructural Analysis of Cementitious Materials. CRC Press, Taylor & Francis Group, Boca Raton, FL.
- [26] Bafarawa, B., Nepryahin, A., Ji, L., Holt, E.M., Wang, J. and Rigby, S.P. (2014) Combining Mercury Thermoporometry with Integrated Gas Sorption and Mercury Porosimetry to Improve Accuracy of Pore-Size Distributions for Disordered Solids. *Journal of Colloid and Interface Science*, **426**, 72-79. <https://doi.org/10.1016/j.jcis.2014.03.053>

- [27] Shi, T., *et al.* (2019) Research Progress on CNTs/CNFs-Modified Cement-Based Composites—A Review. *Construction and Building Materials*, **202**, 290-307. <https://doi.org/10.1016/j.conbuildmat.2019.01.024>
- [28] Hassan, A., Elkady, H. and Shaaban, I.G. (2019) Effect of Adding Carbon Nanotubes on Corrosion Rates and Steel-Concrete Bond. *Scientific Reports*, **9**, Article No. 6285. <https://doi.org/10.1038/s41598-019-42761-2>
- [29] Wang, T., *et al.* (2020) Experimental Study on the Effect of Carbon Nanofiber Content on the Durability of Concrete. *Construction and Building Materials*, **250**, Article ID: 118891. <https://doi.org/10.1016/j.conbuildmat.2020.118891>
- [30] Del Carmen Camacho, M., *et al.* (2014) Mechanical Properties and Durability of CNT Cement Composites. *Materials*, **7**, 1640-1651. <https://doi.org/10.3390/ma7031640>